Dandao Xuebao/Journal of Ballistics
ISSN: 1004-499X
Vol. 35 No. 3 (2023)

Automated Social Distance Recognition and Classification using Seagull Optimization Algorithm with Multilayer Perceptron

Dhanya G Nair[1], Dr. K. P. Sanal Kumar[2*], Dr. S. Anu H Nair[3]

[1]Research Scholar, Department of Computer and Information Science, Annamalai University, Chidambaram, India.
[2]Assistant Professor, P.G Department of Computer Science, R. V. Government Arts College, Chengalpattu, India.
[3]Assistant Professor, Department of CSE, Annamalai University, Chidambaram, India (Deputed to WPT Chennai).
Email:[1]dgn123dhanya@gmail.com, [2]sanalprabha@yahoo.co.in. [3]anu_jul@yahoo.co.in

Abstract

Social distancing (SD) is a set of non-pharmaceutical disease control actions. Its main intention is to stop or decrease the transmission of a spreadable disease. The goal is to decrease the prospect of interaction among peoples who carries an infection and others who are not diseased to diminish disease spread. This can also contain actions like keeping a distance of at least 6 feet from other people, avoiding crowded locations as well as reducing physical communication. The training of SD was suited mainly at the time of COVID-19 virus, where it was suggested as a fundamental action to diminish the spread of disease. The exact rules for SD may differ reliant on the nature of the virus and references from healthcare consultants. SD recognition's main objective is to leverage machine learning (ML) and artificial intelligence (AI) based technical solutions to identify and aware persons when they are not obeying the rules and regulations of SD action. This manuscript offers the design of an Automated Social Distance Recognition and Classification using the Seagull Optimization Algorithm with Multilayer Perceptron (SDRC-SOAMLP) technique. The purpose of the SDRC-SOAMLP technique is to categorize high-risk and low-risk SD using parameter-tuned ML models. To accomplish this, the SDRC-SOAMLP technique initially undergoes two stages of preprocessing: Wiener Filter (WF) based noise removal and Dynamic Histogram Equalization (DHE) based contrast improvement. For the detection and estimation of distance between the pedestrians, the segmentation process involving running average-based adaptive background subtraction and Euclidean distance measurement is used. Followed by, the MLP model can be exploited for the detection and classification of the SD. To enhance the performance of MLP's detection rate, the SOA can be applied for the optimal selection of the parameters related to it. The experimental validation of the SDRC-SOAMLP technique is verified on the SD dataset and the results are examined in distinct measures. The comprehensive comparison study stated the superior performance of the SDRC-SOAMLP model when compared to recent models.

Keywords: Social Distance; Seagull Optimization Algorithm; COVID-19; Multilayer Perceptron; Artificial Intelligence

1. Introduction

Social distancing (SD) can efficiently cover the range of infectious illnesses by decreasing social connections, it might cause financial effects [1]. Disasters like the COVID-19 pandemic generate problems for policymakers because longer-term execution of restricting SD plans causes huge financial harm as well as damage to healthcare schemes [2]. To execute SD, group actions and crowds in meetings, workshops, travel, gatherings, etc. had been completely banned at the time of the quarantine period [3]. People are encouraged to utilize their mobile phones and email for managing and conducting events to reduce the person to person communication [4]. In addition, to cover the transmission of disease, people are informed to implement sanitation measures like washing hands regularly, wearing masks and avoiding close contact with persons who are very ill [5]. But, there is a huge difference between knowing what to prepare to decrease the broadcast of viruses and putting them into training.

Several techniques have been estimated to be capable of aiding authorities or people to monitor as well as obey SD guidelines [6]. For instance, wireless positioning systems efficiently remind persons to preserve a secure space by evaluating distances among people as well as informing them when they are near each other [7]. Besides, other models like Artificial Intelligence (AI) are also employed to simplify or implement SD [8].

Leveraging current wireless techniques in a method of mobile gadgets like tablets, smartphones, laptops and notebooks can improve smart apps that are capable of alerting people whenever the minimum SD need is not followed [9]. In a public location like a university which has many amenities where persons assemble in a classroom, offices, professor hall and canteen, the necessity to obey SD will be more significant and higher. With the aid of smart applications, a virtual fence surrounding the people with the lowest range can be recognized [10].

This manuscript offers the design of an Automated Social Distance Recognition and Classification using the Seagull Optimization Algorithm with Multilayer Perceptron (SDRC-SOAMLP) technique. To accomplish this, the SDRC-SOAMLP technique initially undergoes two stages of preprocessing: Wiener Filter (WF) based noise removal and Dynamic Histogram Equalization (DHE) based contrast improvement. For the detection and estimation of distance between the pedestrians, the segmentation process involving running average-based adaptive background subtraction and Euclidean distance (ED) measurement is used. Followed by, the MLP model can be exploited for the detection and classification of the SD. To enhance the performance of the MLP's detection rate, the SOA can be applied for the optimal selection of the parameters related to it. An experimental validation of the SDRC-SOAMLP technique is verified on the SD dataset and then results are examined in distinct measures.

2. Literature survey

Pandiyan et al. [11] developed a YOLO v3 object detection technique to mechanize the observation of SD amongst people via CCTV. Also, this study employed to identify and track the individual and estimate inter-person space in a gathering below a stimulating atmosphere which contains incomplete prominence, lighting variants, and individual obstruction. Furthermore, the YOLO V3 technique tests with ShuffleNetV2 and Darknet53 backbone framework. Tushar et al. [12] proposed a technique by employing convolutional designs. Initially, the people in video frames are identified with the help of DL. The second stage is to estimate the distance amongst any dual persons over techniques of image processing. The method begins by employing an RGB image of any dimension; the technique employs Predefined Training for the extraction of features. Faster Regional Convolutional Neural Networks (CNNs) have been employed for training.

In [13], the authors develop to integrate IoT and multi-access edge computing (MEC) techniques to construct a service that forms as well as cautions persons in real-time if they are not performing SD. The presented service is poised of a client app side mounted on consumers' smartphones, which sometimes shows GPS organised to remote servers at the control of the system. The remote servers employ a local technique to identify as well as notify consumers who not performing SD. Naji et al. [14] developed a smart ML-based method for observing mask-wearing as well as SD. The presented model is executed for observing people and detecting those who do not obey the instructions of mask-wearing or SD. The study will aid in controlling prevalent, decreasing the spread of COVID-19 and hassle the significance of SD.

Mathurkar et al. [15] presented a social-distancing recognition device. This is mainly completed by observing real-time streams of video from cameras. To offer an effectual clarification, the study proposed a technique which comes with dual stages – initially object recognition stage where individuals will be identified from video streams. Then, screening statistical investigation in a method of dashboards and directing alarms to troubled experts to take required acts. In [16], an energy-efficient adaptive suggestion solution involving a cascade of a modest wake-up trigger and an 8-bit quantized CNN model has been developed, which is only higher for complex to categorize frames. Using such an adaptive method on an IoT Microcontroller, the technique displayed that, when handling an output of an 8×8 low-resolution IR sensor, it is capable of decreasing energy consumption.

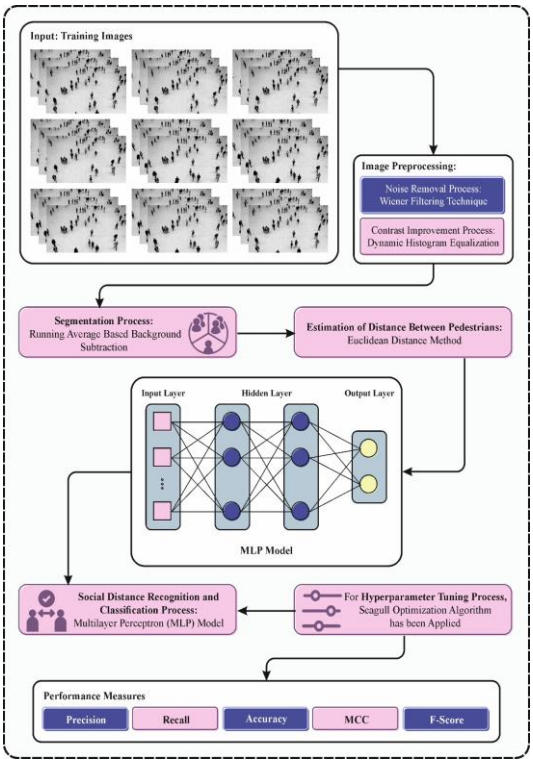

Fig. 1. Workflow of SDRC-SOAMLP technique

3. The Proposed Model

In this manuscript, we offer the design of an automated SDRC-SOAMLP technique. The purpose of the SDRC-SOAMLP technique is to categorize high-risk and low-risk SD using parameter-tuned ML models. The SDRC-SOAMLP technique comprises three major procedures such as pre-processing, segmentation and classification. At the pre-processing stage, the quality of the input images can be enhanced by the use of WF based sound removal and DHE based contrast improvement. Besides, the segmentation process takes place where the Running average based adaptive background subtraction and ED based pedestrian distance calculation are involved. Finally, the SOA with MLP model can be exploited for accurate detection and classification of the SD. Fig. 1 depicts the workflow of SDRC-SOAMLP technique.

3.1. Image Pre-processing

In the initial stage, the WF based pre-processing and DHE based contrast enhancement process is performed to boost the quality of the input images.

3.1.1. WF based Pre-processing

To eradicate the noise in input images, WF based pre-processing is utilized. WF is a complex image preprocessing method used for noise removal [17]. It works in the frequency domain and is aimed at minimizing the mean square error between the filtered image and an original version. WF consider the signal and the noise feature, which makes it very efficient in a scenario where the noise properties are known. By adapting filter parameters based on the local signal and noise features, the WF can considerably improve the visual quality of an image by reducing unwanted noise, contributing to better interpretation and image analysis in different applications.

3.1.2. DHE based Contrast Enhancement

To enhance the dissimilarity level in the images, the DHE approach is applied. DHE is a robust image preprocessing technique intended to improve the visibility and contrast of details within the image [18]. Different from classical histogram equalization, which exploits a static transformation function, DHE applies dynamic and adaptive adjustments based on local image properties. This makes DHE very efficient in scenarios where the image shows variation in illumination or when specific regions have dissimilar contrast levels. By reassigning pixel intensity across the dynamic range based on local histogram characteristics, DHE can improve image clarity, enhance overall visibility, and bring out fine details, which makes it a valuable tool in image processing applications namely computer vision or medical imaging.

3.2. Image Segmentation

Once the input images are pre-processed, the next stage is to perform segmentation to detect the occurrence of pedestrians and estimate the space among them by employing ED.

3.2.1. Running Average based Adaptive Background Subtraction model

Implementing a running average for background subtraction in pedestrian detection includes dynamically updating an average image over time. This technique efficiently isolates moving entities, like pedestrians, against a more stable background by adjusting to environmental changes. The running average, estimated pixel-wise across consecutive frames, allows the management of progressive change in scene or lighting features. Consequent subtraction of this adaptive background from the present frame is used to highlight the foreground object. Particularly, this method is considered beneficial in a real-time scenario where the environmental condition is subjected to fluctuation, providing a basis for reliable accurate and pedestrian detection techniques.

3.2.2. Distance Calculation Using Euclidean Distance

To compute the distance among identified pedestrians, the ED based distance calculation is applied. ED is a popular metric used to calculate the space between binary points in Euclidean space [19]. ED is used for measuring the spatial separation between dissimilar features or points. Now, a couple of scenarios where ED is frequently applied:

Bounding Box Overlap: while identifying the pedestrians, every detected pedestrian is signified as the bounding box. ED is for calculating the spatial separation between the centroid of two bounding boxes:

$$Distance = \sqrt{(x_2 - x_1)^2 + (y_2 - y_1)^2} \qquad (1)$$

This distance is compared to the threshold for determining whether the bounding box overlaps or is closer to the considered part of a similar object.

Feature Space: pedestrians can be determined by the feature vector (representing the color, texture, or shape of the pedestrian). Then, ED is used for measuring the difference between two feature vectors:

$$Distance = \sqrt{\sum_{i=1}^{n} (x_{2i} - x_{1i})^2} \qquad (2)$$

Where n denotes the number of dimensions in feature space. Using ED for pedestrian detection includes a dissimilarity score or a threshold distance. If a computed distance is lesser than the threshold, then two objects are close enough or considered similar.

3.3. MLP based Classification

For accurate detection of SD, the MLP model is used. An input and output vectors are mapped non-linearly through the DL neural network model called MLP which is composed of hidden, input, and output layers [20]. For the neuron activation, MLP exploits a non-linear activation function excepting the input node. MLP can manage data that cannot be separated linearly due to its availability of non-linear functions for activation. The connection weight is modified, and the computation considers the actual and desired outputs. The output node is represented as y at n^{th} data point:

$$e_y(n) = t_y(n) - p_y(n) \tag{3}$$

Here t indicates the target value and p denotes the output of perceptron.

Node weight is changed to diminish the inaccuracy of total output.

$$\in (n) = \frac{1}{2}\sum_{y} \quad e2y(n) \tag{4}$$

Using gradient descent, any change in the weight is given as follows.

$$\Delta w_{yx}(n) = \eta \frac{\delta\epsilon(n)}{\left(\delta v_y(n)\right)} p_x(n) \tag{5}$$

Now η denotes the learning rate and p_x indicates the output of prior neuron.

Derivation computation can be evaluated by vy, which is an induced local field.

$$\frac{\delta\epsilon(n)}{\left(\delta v_y(n)\right)} = e_y(n)\phi'\left(v_y(n)\right) \tag{6}$$

In Eq. (6), ϕ refers to the derivative of the constant activation function.

$$\frac{\delta\epsilon(n)}{(\delta v_y(n))} = e_y(n)\sum_{k} \quad \frac{\delta\epsilon(n)}{\left(\delta v_y(n)\right)} w_{ky}(n) \tag{7}$$

3.4. SOA based Parameter Tuning

Finally, the SOA algorithm adjusts the parameters related to the SVM model. Exploration (migration) and exploitation are the essentials of the SOA mathematical technique [21]. During exploration, this method can fulfil 3 conditions (collision avoidance, shift from the direction of optimum neighbour, and staying near the optimum searching agent) for replicating that group of seagulls moves around. The migration behaviour is demonstrated by the subsequent formula:

$$\overrightarrow{D_s} = \left|A \times \overrightarrow{X_s}(t) + B \times \left(\overrightarrow{X_{bs}}(t) - \overrightarrow{X_s}(t)\right)\right| \tag{8}$$

$$A = fc - \left(iter \times \left(\frac{fc}{Max\_iter}\right)\right) \tag{9}$$

$$B = 2 \times A^2 \times rand \tag{10}$$

Whereas, the distance between the present searching agent and an optimum search agent has been represented by $\vec{D}_s$,$\vec{X}_s(t)$ implies the existing place of the searching agent, $\vec{X}_{bs}(t)$ stands for the location of the best-fit searching agent. t designates an existing iteration, A signifies the linear reduction from fc to 0, B refers to the random parameter that makes sure that it modifies the balance of exploitation and exploration.

During exploitation, seagull seeks to utilize the history and experience of the search process. Seagull uses their wings and weight to retain their height. The search agent updates the location based on the optimum search agent. Consequently, the subsequent formula is utilized for determining the updated location of the search agent:

$$\overrightarrow{X_s}(t+1) = \left(\overrightarrow{D_s} \times X' \times Y' \times Z'\right) + \overrightarrow{X_{bs}}(t) \quad (11)$$

In Eq. (11), $\vec{X}_s(t+1)$ is the location updating of the other search agents. X', Y' and Z' indicates the curved effort that behavior delivers in the air:

$$k = pi.rand \quad (12)$$

$$r = u.e^{kv} \quad (13)$$

$$X' = r.cos(k) \quad (14)$$

$$Y' = r.sin(k) \quad (15)$$

$$Z' = r.k \quad (16)$$

The radius of the spiral turn is r, k is a randomly generated number within $[0,2\pi]$. e shows the natural logarithms base, u and v are constants that define the spiral method. Fig. 2 illustrates the flowchart of SOA.

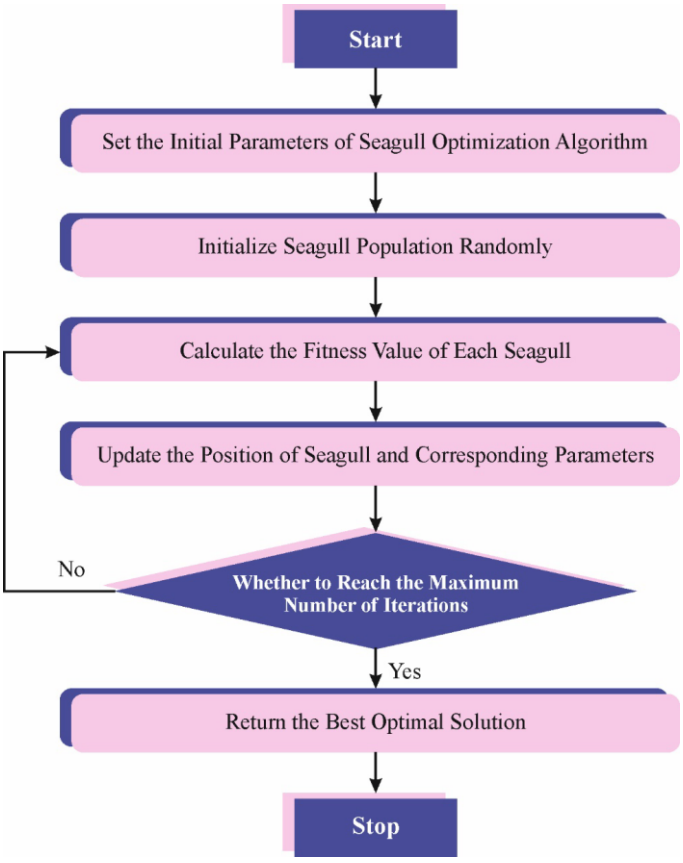

Fig. 2. Flowchart of SOA

Algorithm: Pseudocode of SOA

Input: seagull population $P_s^{\rightarrow}$
Output: Optimum search agent $P_{bs}^{\rightarrow}$
Procedure SOA
Initialize the parameters, fc, and $Max\_iteration$
While ($t < Max\_iteration$)
$P_{bs}^{\rightarrow} \leftarrow ComputeFitness(P_s^{\rightarrow})$
$rd \leftarrow$Rand (0,1)
$k \leftarrow$Rand $(0,2\pi)$
$r \leftarrow u \times e^{kv}$
Compute the distance $D_s^{\rightarrow}$ using Eq. (8)
$P \leftarrow x' \times y' \times z'$
$P_s^{\rightarrow}(x) \leftarrow (D_s^{\rightarrow} \times P) + P_{bs}^{\rightarrow}$
$t \leftarrow t + 1$
End while
Return $P_{bs}^{\rightarrow}$
End process
Procedure ComputeFitness ($P_s^{\rightarrow}$)
For $i \leftarrow 1$ to ndo
$FITs[i] \leftarrow FitnessFucntion\left(P_s^{\rightarrow}(i,:)\right)$
End for
$FITsbest \leftarrow BEST(FITs[])$
return FITsbest
End process
Procedure BEST(FITs[])
Best $\leftarrow FITs[0]$
For $i \leftarrow 1$ to n do
if (FITs $[i]$ <Best) then Best $\leftarrow FlTs[i]$
end if
end for
return Best
End process

The fitness selection is the significant factor manipulating the act of the SOA method. The hyperparameter range procedure includes the solution encoding tactic to estimate the candidate solution effectiveness. In this work, the SOA reflects accuracy as the foremost measure to propose the fitness function that is expressed as follows.

$$Fitness = max(P) \tag{17}$$

$$P = \frac{TP}{TP + FP} \tag{18}$$

From above mentioned expression, FP indicates the false positive value and TP means the true positive value.

4. Performances validation

The SD detection outcomes of the SDRC-SOAMLP model are verified using SD dataset. The dataset [22] includes 1000 samples with two class labels as represented in Table 1.

Table 1 Details of dataset

Class	No. of Instances
High_Risk	500
Low_Risk	500
Total Instances	**1000**

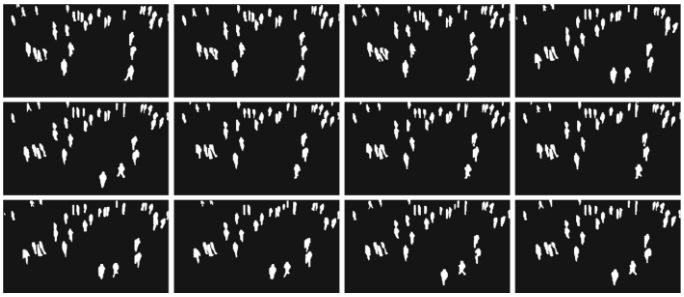

Fig. 3. Segmented Regions

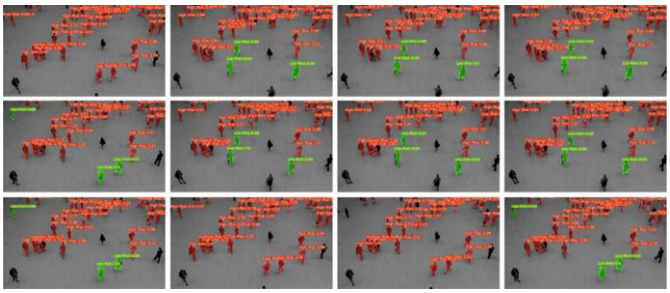

Fig. 4. Detection Regions

Fig. 3 shows the segmented regions obtained by the SDRC-SOAMLP technique and the corresponding SD detected regions are shown in Fig. 4. These results ensure that the SDRC-SOAMLP technique accurately recognized the SD classes.

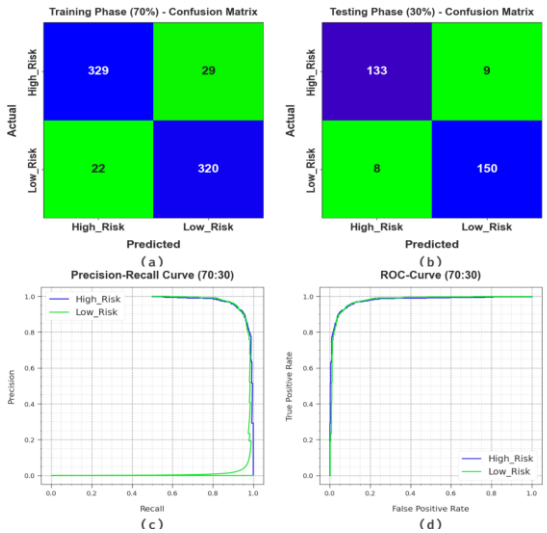

Fig. 5. 70:30 of TRPH/TSPH of (a-b) Confusion matrices (c) PR-curve and (d) ROC-curve

Fig. 5 validates the classifier outcomes of SDRC-SOAMLP model on 70:30 of TRPH/TSPH. Figs. 5a-5b portrays the confusion matrices presented by the SDRC-SOAMLP technique. The figure indicated that the SDRC-SOAMLP method exactly detected as well as categorized with high_risk and low_risk classes. Similarly, Fig. 5c validates the PR study of SDRC-SOAMLP methodology. The figure described that the SDRC-SOAMLP approach has gained maximum PR performance below all classes. Finally, Fig. 5d exemplifies the ROC study of the SDRC-SOAMLP method. The figure represented that the SDRC-SOAMLP technique has outcome in proficient results with maximum ROC values below different class labels.

In Table 2 and Fig. 6, the SD detection results obtained by the SDRC-SOAMLP technique on 70:30 of TRPH/TSPH are demonstrated. The results showcase the enhanced performance of the SDRC-SOAMLP technique in the SD detection process. With 70% of TRPH, the SDRC-SOAMLP system provides an average $accu_y$, $prec_n$, $reca_l$, F_{score}, and MCC of 92.73%, 92.71%, 92.73%, 92.71%, and 85.44%, respectively. Meanwhile, on 30% of TSPH, the SDRC-SOAMLP model provides an average $accu_y$, $prec_n$, $reca_l$, F_{score}, and MCC of 94.30%, 94.33%, 94.30%, 94.32%, and 88.63%, respectively.

Table 2 SD detection outcomes of the SDRC-SOAMLP method under 70:30 of TRPH/TSPH

Classes	$Accu_y$	$Prec_n$	$Reca_l$	F_{score}	***MCC***
TRPH (70%)					
High_Risk	91.90	93.73	91.90	92.81	85.44
Low_Risk	93.57	91.69	93.57	92.62	85.44
Average	**92.73**	**92.71**	**92.73**	**92.71**	**85.44**
TSPH (30%)					
High_Risk	93.66	94.33	93.66	93.99	88.63
Low_Risk	94.94	94.34	94.94	94.64	88.63
Average	**94.30**	**94.33**	**94.30**	**94.32**	**88.63**

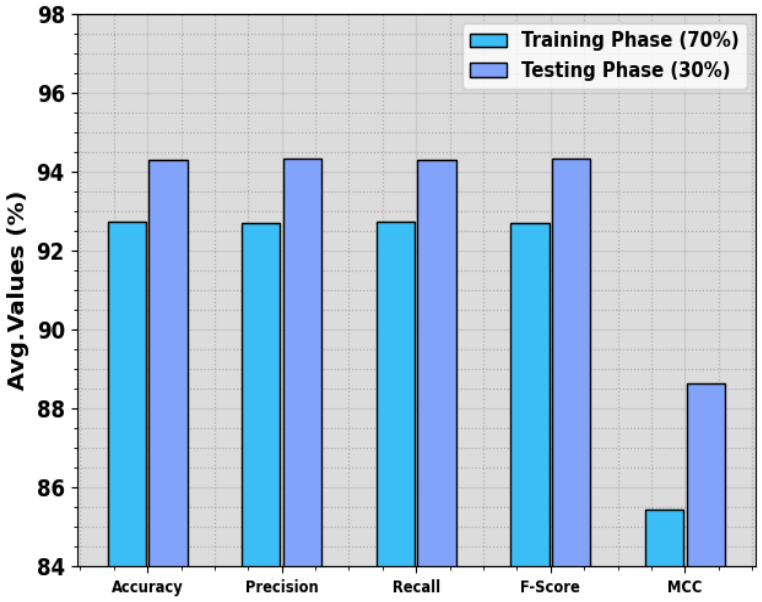

Fig. 6. Average outcomes of the SDRC-SOAMLP model on 70:30 of TRPH/TSPH

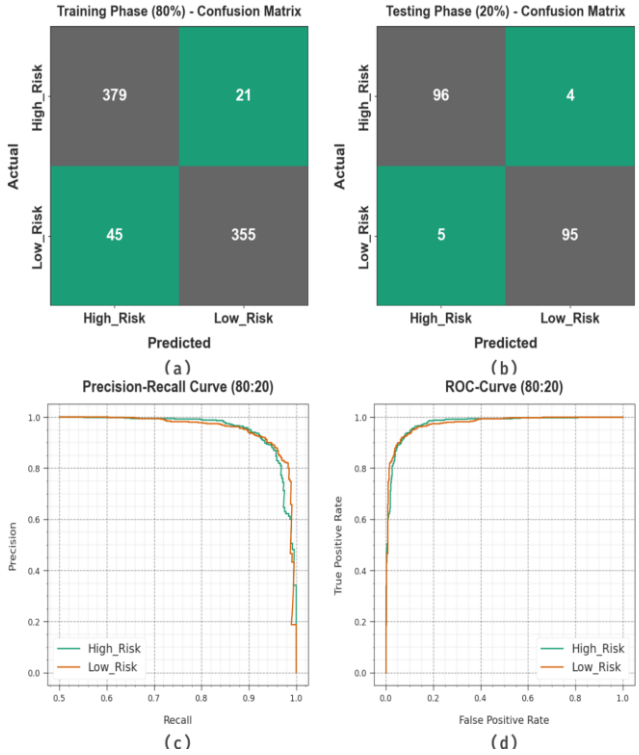

Fig. 7. 80:20 of TRPH/TSPH of (a-b) Confusion matrices (c) PR-curve and (d) ROC-curve

Fig. 7 proves the classifier results of SDRC-SOAMLP model on 80:20 of TRPH/TSPH. Figs. 7a-7b depicts the confusion matrices that offered by the SDRC-SOAMLP model. The figure signified that the SDRC-SOAMLP technique has correctly detected as well as classified with high_risk and low_risk classes. Also, Fig. 7c validates the PR examination of SDRC-SOAMLP technique. The figure conveyed that the SDRC-SOAMLP model has gained extreme PR performance below all classes. Lastly, Fig. 7d validates the ROC study of SDRC-SOAMLP model. The figure shows that the SDRC-SOAMLP approach has resulted in proficient results by maximum ROC values below separate class labels.

In Table 3 and Fig. 8, the SD recognition results gained by the SDRC-SOAMLP method on 80:20 of TRPH/TSPH are established. The results showcase the improved performance of the SDRC-SOAMLP system on the SD recognition procedure. With 80% of TRPH, the SDRC-SOAMLP model delivers an average $accu_y$, $prec_n$, $reca_l$, F_{score}, and MCC of 91.75%, 91.90%, 91.75%, 91.74%, and 83.65%. Similarly, on 20% of TSPH, the SDRC-SOAMLP approach provides an average $accu_y$, $prec_n$, $reca_l$, F_{score}, and MCC of 95.50%, 95.50%, 95.50%, 95.50%, and 91.00%, separately.

Table 3 SD detection analysis of the SDRC-SOAMLP method under 80:20 of TRPH/TSPH

Classes	$Accu_y$	$Prec_n$	$Reca_l$	F_{score}	***MCC***
TRPH (80%)					
High_Risk	94.75	89.39	94.75	91.99	83.65
Low_Risk	88.75	94.41	88.75	91.49	83.65
Average	**91.75**	**91.90**	**91.75**	**91.74**	**83.65**
TSPH (20%)					
High_Risk	96.00	95.05	96.00	95.52	91.00
Low_Risk	95.00	95.96	95.00	95.48	91.00
Average	**95.50**	**95.50**	**95.50**	**95.50**	**91.00**

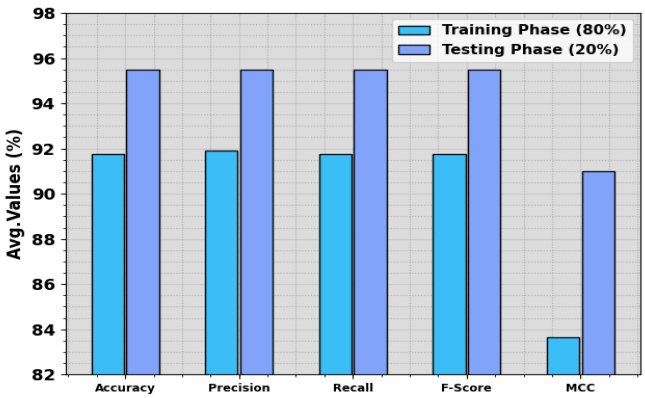

Fig. 8. Average outcomes of the SDRC-SOAMLP algorithm on 80:20 of TRPH/TSPH

To further validate the betterment of the SDRC-SOAMLP technique, a wide-ranging comparison study is given in Table 4 and Fig. 9 [23]. The results demonstrated that the SDRC-SOAMLP method shows capable performance over other techniques. Depend on $accu_y$, the SDRC-SOAMLP technique offers increasing $accu_y$ of 95.50% whereas the CNN, MobileNet, Inception v3, ResNet-50, RF, LR, and Stacked ResNet-50 models resulted in reduced $accu_y$ of 75%, 83%, 83%, 77%, 82.30%, 82.98%, and 87%, respectively.

Table 4 Comparison analysis of the SDRC-SOAMLP model with other approaches

Model	$Accu_y$	$Prec_n$	$Reca_l$	F_{score}
CNN Model	75.00	51.00	65.00	52.00
MobileNet V3	83.00	56.00	93.00	59.00
Inception V3	83.00	66.00	93.00	65.00
ResNet-50 Model	77.00	54.00	67.00	59.00
Random Forest Model	82.30	64.40	90.27	71.23
Logistic Regression Model	82.98	69.12	90.54	74.57
Stacked ResNet-50	87.00	71.00	92.00	79.00
SDRC-SOAMLP	95.50	95.50	95.50	95.50

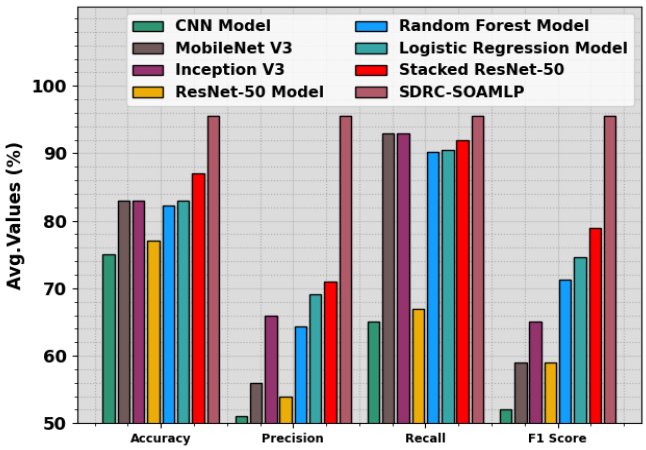

Fig. 9. Comparison analysis of the SDRC-SOAMLP system with other models

Also, on $prec_n$ the SDRC-SOAMLP model provides growing $prec_n$ of 95.50% while the CNN, MobileNet, Inception v3, ResNet-50, RF, LR, and Stacked ResNet-50 approaches resulted in decreased $prec_n$ of 51%, 56%, 66%, 54%, 64.40%, 69.12%, and 71%. Moreover, with $reca_l$ the SDRC-SOAMLP method provides increasing $reca_l$ of 95.50% but the CNN, MobileNet, Inception v3, ResNet-50, RF, LR, and Stacked ResNet-50 techniques resulted in decreased $reca_l$ of 65%, 93%, 93%, 67%, 90.27%, 90.54%, and 92%, correspondingly.

Table 5 CT analysis of the SDRC-SOAMLP model with other methods

Model	**Computational Time (sec)**
CNN Model	5.52
MobileNet V3	3.86
Inception V3	3.52
ResNet-50 Model	3.30
Random Forest Model	4.77
Logistic Regression Model	4.29
Stacked ResNet-50	4.13
SDRC-SOAMLP	2.03

Finally, the comprehensive comparative computation time (CT) results of the SDRC-SOAMLP technique are depicted in Table 5 and Fig. 10. The results highlighted the better performance of the SDRC-SOAMLP technique with the least CT of 2.03s. On the other hand, the CNN, MobileNet, Inception v3, ResNet-50, RF, LR, and Stacked ResNet-50 models obtain increased CT values of 5.52s, 3.86s, 3.52s, 3.30s, 4.77s, 4.29s, and 4.13s. These results safeguarded the enhanced detection act of the SDRC-SOAMLP model in terms of different metrics.

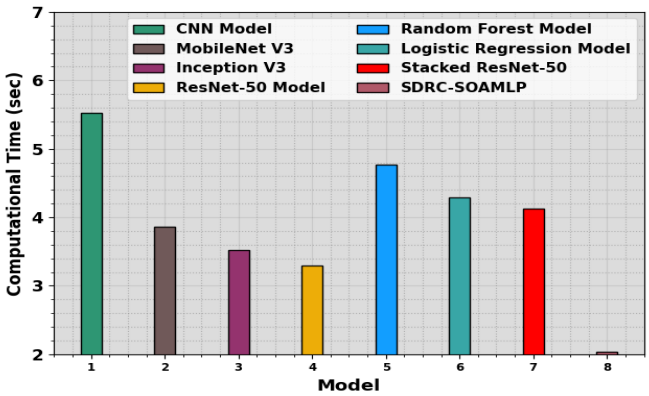

Fig. 10. CT outcome of the SDRC-SOAMLP algorithm with other existing systems

5. Conclusion

In this manuscript, we offer the design of an automated SDRC-SOAMLP technique. The purpose of the SDRC-SOAMLP technique is to categorize high-risk and low-risk SD using parameter tuned ML models. The SDRC-SOAMLP technique comprises three major procedures like pre-processing, segmentation and classification. In the pre-processing phase, the excellence of the input images can be enhanced by the use of WF based noise removal and DHE based contrast improvement. Moreover, the segmentation process takes place where the Running Average based adaptive background subtraction and Euclidean distance based pedestrian distance calculation are involved. At last, the SOA with MLP model can be exploited for accurate detection and classification of the SD. An experimental validation of the SDRC-SOAMLP technique is verified on the SD

dataset and then results are examined in distinct measures. The comprehensive comparison study stated the better performance of the SDRC-SOAMLP methodology compared to recent models.

References

[1] Vinitha, V., Velantina, V.: Social distancing detection system with artifcial intelligence using computer vision and deep learning. Int. Res. J. Eng. Technol. (IRJET) 7(8), 4049–4053 (2020)

[2] Ainslie KE, Walters CE, Fu H, Bhatia S, Wang H, Xi X, et al. Evidence of initial success for China exiting COVID-19 social distancing policy after achieving containment. Wellcome Open Research. 2020; 5.

[3] Rezaei, M., Azarmi, M.: DeepSOCIAL: social distancing monitoring and infection risk assessment in COVID-19 pandemic. Appl. Sci. 10(7514), 1–29 (2020)

[4] Saponara, S., Elhanashi, A., Gagliardi, A.: Implementing a real-time, AI based, people detection and social distancing measuring system for Covid-19. J. Real-Time Image Process. 18(6), 1937– 1947 (2021)

[5] Arya, S., Patil, L., Wadeganokar, A., et al.: Study of various measure to monitor social distancing using computer vision: a review. Int. J. Eng. Res. Technol. (IJERT) 10(5), 329–326 (2021)

[6] Prem K, Liu Y, Russell TW, Kucharski AJ, Eggo RM, Davies N, et al. The effect of control strategies to reduce social mixing on outcomes of the COVID-19 epidemic in Wuhan, China: a modelling study. The Lancet Public Health. 2020

[7] Cobb J, Seale M. Examining the effect of social distancing on the compound growth rate of SARS-CoV2 at the county level (United States) using statistical analyses and a random forest machine learning model. Public Health. 202

[8] Yang, D., Yurtsever, E., Renganathan, V., et al.: A vision-based social distancing and critical density detection system for COVID-19. Sensors 21(4608), 1–15 (2021)

[9] Punn NS, Sonbhadra SK, Agarwal S. Monitoring COVID-19 social distancing with person detection and tracking via fine-tuned YOLO v3 and Deepsort techniques. arXiv preprint arXiv:200501385. 2020.

[10] Adolph C, Amano K, Bang-Jensen B, Fullman N, Wilkerson J. Pandemic politics: Timing state-level social distancing responses to COVID-19. medRxiv. 2020.

[11] Pandiyan, P., Thangaraj, R., Subramanian, M., Rahul, R., Nishanth, M. and Palanisamy, I., 2022. Real-time monitoring of social distancing with person marking and tracking system using YOLO V3 model. *International Journal of Sensor Networks*, *38*(3), pp.154-165.

[12] Tushar, B.M., Rahman, M.S., Jaffer, A.S. and Indumathy, M., 2023. Face Mask and Social Distancing Detection Using Faster Regional Convolutional Neural Network. *Advances in Science and Technology*, *124*, pp.96-102.

[13] Ksentini, A. and Brik, B., 2020. An edge-based social distancing detection service to mitigate covid-19 propagation. *IEEE Internet of Things Magazine*, *3*(3), pp.35-39.

[14] Naji, M.F., Joumaa, C., Alswailem, Y., Alobthni, A. and Albusilan, R., 2022, June. Machine Learning-based System for Monitoring Social Distancing and Mask Wearing. In *2022 IEEE World AI IoT Congress (AIIoT)* (pp. 001-008). IEEE.

[15] Mathurkar, G., Parkhi, C., Utekar, M. and Chitte, P.H., 2021. Ensuring social distancing using machine learning. In *ITM Web of Conferences* (Vol. 40, p. 03049). EDP Sciences.

[16] Xie, C., Pagliari, D.J. and Calimera, A., 2022, June. Energy-efficient and Privacy-aware Social Distance Monitoring with Low-resolution Infrared Sensors and Adaptive Inference. In *2022 17th Conference on Ph. D Research in Microelectronics and Electronics (PRIME)* (pp. 181-184). IEEE.

[17] Ferzo, B.M. and Mustafa, F.M., 2020, April. Image Denoising in Wavelet Domain Based on Thresholding with Applying Wiener Filter. In *2020 International Conference on Computer Science and Software Engineering (CSASE)* (pp. 106-111). IEEE.

[18] Rao, B.S., 2020. Dynamic histogram equalization for contrast enhancement for digital images. *Applied Soft Computing*, *89*, p.106114.

[19] Yang, Y., Cai, J., Yang, H. and Zhao, X., 2022. Density clustering with divergence distance and automatic center selection. *Information Sciences*, *596*, pp.414-438.

[20] Juna, A., Umer, M., Sadiq, S., Karamti, H., Eshmawi, A.A., Mohamed, A. and Ashraf, I., 2022. Water quality prediction using KNN imputer and multilayer perceptron. *Water*, *14*(17), p.2592.

[21] Chalh, A., Chaibi, R., Hammoumi, A.E., Motahhir, S., Ghzizal, A.E. and Al-Dhaifallah, M., 2022. A novel MPPT design based on the seagull optimization algorithm for photovoltaic systems operating under partial shading. *Scientific Reports*, *12*(1), p.21804.

[22] https://github.com/ChargedMonk/Social-Distancing-using-YOLOv5

[23] Walia, I.S., Kumar, D., Sharma, K., Hemanth, J.D. and Popescu, D.E., 2021. An integrated approach for monitoring social distancing and face mask detection using stacked Resnet-50 and YOLOv5. *Electronics*, *10*(23), p.2996.